Am J Transl Res 2023;15(7):4829-4850
www.ajtr.org /ISSN:1943-8141/AJTR0150800

Original Article

Characterization of ferroptosis driver gene signature in head and neck squamous cell carcinoma (HNSC)

Khalida Shaikh[1], Yusra Iqbal[2], Mostafa A Abdel-Maksoud[3], Amina Murad[4], Nadia Badar[5], Khaloud Mohammed Alarjani[3], Komal Siddiqui[6], Khushboo Chandio[7], Taghreed N Almanaa[7], Muhammad Jamil[8], Mubarik Ali[9], Norina Jabeen[10], Ahmed M Hussein[11,12]

[1]Liaquat University of Medical and Health Sciences, Jamshoro, Pakistan; [2]Continental Medical College Lahore, Lahore 54660, Pakistan; [3]Botany and Microbiology Department, College of Science, King Saud University, Riyadh 11451, Saudi Arabia; [4]Department of Bioscience, Comsats University, Islamabad, Pakistan; [5]Department of Medical Oncology Allied Hospital, Faisalabad, Pakistan; [6]Institute of Biotechnology and Genetic Engineering University of Sindh, Jamshoro, Pakistan; [7]Peoples Nursing School LUMHS, Jamshoro, Pakistan; [8]PARC Arid Zone Research Centre, Dera Ismail Khan 29050, Pakistan; [9]Animal Science Institute, National Agricultural Research Center, Islamabad 54000, Pakistan; [10]Department of Rural Sociology, University of Agriculture, Faisalabad 38000, Pakistan; [11]Department of Pharmaceutical Sciences, Division of Pharmacology and Toxicology, University of Vienna, 1090 Vienna, Austria; [12]Programme for Proteomics, Paracelsus Medical University, Salzburg, Austria

Received April 19, 2023; Accepted June 29, 2023; Epub July 15, 2023; Published July 30, 2023

Abstract: Background: Head and neck squamous cell carcinoma (HNSC), a prevalent malignant tumor with a low survival rate, is often accompanied by ferroptosis, which is a recently-described type ofprogrammed cell death. Investigating the significance of ferroptosis driver genes in HNSC, this study aimed to assess their diagnostic and prognostic values, as well as their impact on treatment and tumor immune function. The results of this investigation provide novel insight into using ferroptosis-related genes as molecular biomarkers as well as precise chemotherapeutic targets for the therapy of HNSC. Methodology: A detailed in silico and in vitro experiment-based methodology was adopted to achieve the goals. Results: A total of 233 ferroptosis driver genes were downloaded from the FerrDB database. After comprehensively analyzing these 233 ferroptosis driver genes by various TCGA databases, RNA-sequencing (RNA-seq), and Reverse Transcription Quantitative Real-Time Polymerase Chain Reaction (RT-qPCR) techniques, TP53 (tumor protein 53), PTEN (Phosphatase and TENsin homolog deleted on chromosome 10), KRAS (Ki-ras2 Kirsten rat sarcoma viral oncogene homolog), and HRAS (Harvey Rat sarcoma virus) were identified as differentially expressed hub genes. Interestingly, these hub genes were found to have significant ($P < 0.05$) variations in their mRNA and protein expressions and effects on overall survival of the HNSC patients. Moreover, targeted bisulfite-sequencing (bisulfite-seq) analysis revealed that promoter hypomethylation pattern was associated with up-regulation of hub genes (TP53, PTEN, KRAS, and HRAS). In addition to this, hub genes were involved in diverse oncogenic pathways. Conclusion: Since HNSC pathogenesis is a complex process, using ferroptosis driver hub genes (TP53, PTEN, KRAS, and HRAS) as a diagnostic and prognostic tool, and therapeutically targeting those genes through appropriate drugs could bring a milestone change in the drug discovery and management and survival in HNSC.

Keywords: HNSC, ferroptosis, chemotherapy, overall survival

Introduction

Head and neck cancer (HNSC) is a group of diseases that originate in different regions of the head and neck, such as the mouth, nose, throat, larynx, and salivary glands [1]. The incidence of HNSC varies globally, with a higher prevalence in developing countries, particularly in South and Southeast Asia, due to high tobacco and alcohol consumption [2]. In developed countries, such as North America and Europe, the incidence of HNSC has decreased over the years, primarily due to a reduction in tobacco use [3]. However, the prevalence of human papillomavirus (HPV) associated with HNSC has increased, particularly in young adults, which underscores the importance of awareness, prevention, and early detection [4].

HNSC often presents with symptoms such as neck lumps, persistent sore throat or hoarseness, difficulty in swallowing or breathing, pain or numbness around the mouth or neck, among others [5]. These symptoms may vary depending on the location of the cancer, and early diagnosis is essential in improving treatment outcomes. The prognosis for HNSC largely depends on the stage of the disease at the time of diagnosis, with early-stage tumors being easier to treat and having a better prognosis than late-stage tumors [6].

Ferroptosis is a type of regulated cell death that is characterized by the accumulation of iron and lipid peroxidation [7]. It is a unique form of cell death that occurs through oxidative stress caused by the accumulation of reactive oxygen species (ROS) [8]. While apoptosis and necrosis are the two main types of cell death, ferroptosis is distinct in its molecular mechanism, morphology, and physiologic functions [9]. Ferroptosis has been implicated in many different diseases, including cancer, neurodegenerative disorders, and organ failure [10]. Additionally, manipulation of ferroptotic pathways has been shown to be an effective strategy for cancer treatment since cancer cells have elevated iron levels and are more susceptible to ferroptosis induction [9].

In recent times, there has been an increased focus on identifying biomarkers of ferroptosis at multiple levels, including morphology, protein, gene, and biochemistry [11]. In this regard, Lin et al. explored the possibility of the SLE7A11 gene serving as biomarker for ferroptosis in HNSC and colorectal cancer patients [12]. Moreover, Lu et al. constructed a long non-coding RNA signature-based panel to predict the prognosis of HNSC patients [13]. Nonetheless, detecting dependable ferroptosis-related molecular biomarkers in HNSC continues to be a challenge.

The focus of this report was on analyzing various ferroptosis driver genes in HNSC patients for developing reliable diagnostic and prognostic models of some valuable genes. To achieve this, we sourced data from FerrDB (http://www.zhounan.org/ferrdb/current/) database and conducted a series of in silico and in vitro analyses to identify cutting-edge ferroptosis-related important molecular markers in HNSC patients. This study demonstrated that the identified ferroptosis-related molecular biomarkers were closely related to HNSC development and have effects on the prognosis of HNSC patients.

Methodology

Data source, DEGs, PPI, module, and hub gene analysis

A total of 233 ferroptosis driver genes were downloaded from the FerrDB database. The FerrDB is the first of its kind in the world that focuses on ferroptosis regulators and ferroptosis-disease associations.

The STRING (Search Tool for the Retrieval of Interacting Genes/Proteins) database is a valuable and comprehensive resource for researchers studying molecular interactions and functional relationships. With data gathered from hundreds of organisms and multiple sources including experimental evidence, text-mining, and computational predictions, STRING offers a wealth of information on protein-protein interactions (PPIs), as well as gene co-expression and functional associations. The database enables users to build interaction networks, visualize data, and analyze results, helping to streamline research and support discovery. A PPI of the obtained 233 ferroptosis driver genes was developed in order to get the depth of closeness among genes through STRING database [14]. The PPI was developed with a confidence score of 0.700 as a threshold value. For all other parameters, STRING database was used with default setting.

The developed PPI was then retrieved from the STRING database in gto.tsv format and shifted to Cytoscape, version 3.8 [15] for the module and hub gene analyses. Cytoscape software is a bioinformatics tool that allows for the visualization and analysis of complex networks within biological systems. With the help of this tool, researchers are able to create and edit complex network diagrams, perform data integration, and carry out various computational analyses. The MCODE [16] analysis of the retrieved PPI was conducted with default setting for module analysis. Then, Cytohubba [16] analysis helped to determine hub genes based on the degree scores.

Hub gene expressions in TCGA datasets

UALCAN (University of ALabama at Birmingham CANcer) database is an interactive web portal

that enables researchers to analyze and visualize the gene expression data of various cancer types from The Cancer Genome Atlas (TCGA) dataset [17]. It allows users to investigate the differential expression of genes across different types of tumors. In the present study, the mRNA and protein expressions of the hub genes in normal and HNSC samples were presented analyzed by UALCAN and presented in the form of boxplots.

Clinical parameter analysis

The UALCAN tool enables clinical parameter-specific expression analysis for numerous cancer tissues, with corresponding normal control samples [17]. By utilizing the TCGA expression module of UALCAN, correlations between hub genes and varying clinical data were investigated in patients with HNSC.

Expression validation, prognostic, and methylation analyses

For validating hub gene expression on more HNSC TCGA datasets, we next used TCGA expression modules of the GEPIA [18], OncoDb [19], and GENT2 [20] databases. These databases are designed for storing cancer genomic and transcriptomic data that can be accessed through a web interface. These web sources allow researchers to conduct data analysis by integrating various data types. Moreover, these databases help researchers conduct hypothesis-driven research that can expedite the process of cancer diagnosis and treatment. Furthermore, to conduct a prognostic analysis, we utilized the "survival module" of the GEPIA database. For the analysis of methylation in the hub genes present in samples of HNSC and controls, we employed the "methylation modules" of MEXPRESS [21] and OcoDB [19].

Mutation status and effect of mutations on the survival of HNSC patients

cBioPortal is a web-based platform that provides a comprehensive and easy-to-use interface for exploring and visualizing cancer genomic data [22]. Developed primarily for cancer researchers, cBioPortal enables them to access a vast array of genomic data and related clinical information, curated from various sources, in a user-friendly and intuitive manner. It allows researchers to browse through genetic alterations, analyze patient data, and compare results across different datasets. In this study, the mutational profiling of the hub genes and determination of the possible impact of the mutations on the survival of HNSC patients was done with the help this database using all HNSC TCGA datasets, available in this database.

Sub-cellular localization and protein expression validation

The Human Protein Atlas (HPA) database has revolutionized the way scientists and researchers approach the study of human proteins [23]. The database contains a comprehensive resource of information about protein expression across a wide range of tissues and cell lines. Through these comprehensive data, researchers can study the function of human proteins and better understand how they interact with each other. This information is essential for developing new drugs, diagnosing diseases, and identifying potential therapeutic targets. Sub-cellular localization and immunohistochemistry (IHC)-based protein expression outcomes of the hub genes in HNSC and control samples were determined with the help of HPA.

Development of a hub gene-based prognostic model

The least absolute shrinkage and selection operator (Lasso) and multivariate Cox proportional hazard regression analysis were further developed to construct a prediction model with "survival" package in R language [24]. In this analysis, TCGA-HNSC dataset was used a training dataset while GSE75538, GSE65858, and E_MTAB_8588 datasets were used as the validation datasets. The formula of the prognostic model of HNSC patients' prognosis was as follows: risk score = the sum of the multivariate Cox regression coefficient variation of each mRNA.

Gene enrichment analysis

DAVID (Database for Annotation, Visualization and Integrated Discovery) is a bioinformatics tool that aids in the functional interpretation of large, complex datasets generated from high-throughput experimentations such as microarrays, proteomics, and genomics. It integrates biological information from different sources

and provides an intuitive interface for the discovery and visualization of gene ontology, biological pathways, and functional enrichment analysis. DAVID offers various analysis tools, such as clustering, gene set enrichment analysis, and functional annotation tools that enable researchers to generate biologically meaningful results from large heterogeneous datasets. DAVID tool was used in this work to detect the hub gene-enriched functional and pathway terms.

Immune cells infiltration analysis

TIMER (Tumor Immune Estimation Resource) database [25] provides a comprehensive resource for analyzing the immune infiltrates of tumors. This database contains a vast amount of transcriptomic data from over 10,000 tumors across 32 cancer types. Through TIMER, researchers can analyze the immune cells. Overall, TIMER is an essential database for researchers who are interested in understanding the immunologic profile of tumors and its potential impact on cancer progression and treatment. This database was used in the present work for investigating relationships among infiltration levels of the immune cells (CD8+ T cells, CD4+ T cells, and macrophages) and expression levels of the hub genes in HNSC patients.

MicroRNA (miRNA) network and drug prediction analyses

To gain understanding about the miRNA network of the hub genes, we employed the ENCORI database to construct it [26]. In order to utilize the hub genes as therapeutic targets, we probed the DrugBank database for predicting drug interactions with the hub genes [27].

RNA-seq and targeted bisulfite-seq analyses based in vitro validation of the hub gene expression and methylation levels

A total of one HNSC cell line, including FaDu, and one normal human oral keratinocyte (HOK) cell line were purchased from the ATCC (American Type Culture Collection). The purchased cell lines were cultured in DMEM (HyClone), supplemented with 10% fetal bovine serum (FBS; TBD), 1% glutamine, and 1% penicillin-streptomycin in 5% CO_2 at 37°C. Total RNA extraction from all these three cell lines was done using TRIzol® reagent method [28], and the RNA samples were sent to Beijing Genomics Institute (BGI) company for RNA-sequencing analysis.

RNA sequencing (RNA-seq) and targeted bisulfite sequencing (targeted bisulfite-seq) analysis: RNA and DNA samples were sent to Beijing Genomics Institute (BGI) company for RNA-seq bisulfite-seq analysis. Following RNA-seq and targeted bisulfite-seq analyses, the gene expression values of the hub genes were normalized using reads per kilo base million reads (RPKM) and fragments per kilo base million reads (FPKM). The methylation values were normalized as beta values. The obtained FPKM, and beta values against hub genes in HNSC and normal control cell line were compared to identify differences in the expression and methylation levels.

RT-qPCR validation analysis

The specific protocols are as follows: First, the PrimeScript™ RT reagent kit (Takara, Japan) was used for reverse transcription of the extracted RNA from HOK and FaDu cell lines into complementary DNA. Then, the RT-qPCR was carried out on an ABI ViiA 7 Real Time PCR System (Thermo Fisher, USA) with a SuperReal SYBR Green Premix Plus (Tiangen Biotech, China) as a fluorescent dye. GAPDH was used as the internal reference in the present study. All the experiments were done in triplicate independently. All the primers of each hub gene are shown as follows. The $2^{-\Delta\Delta Ct}$ method was employed to evaluate the relative expression of each hub gene [29].

GAPDHF 5'-ACCCACTCCTCCACCTTTGAC-3', GAPDHR 5'-CTGTTGCTGTAGCCAAATTCG-3' [30].

TP53F 5'-CCCCTCCATCCTTTCTTCTC, TP53R 5'-ATGAGCCAGATCAGGGACTG-3' [31].

PTENF 5'-TGGCATACACCAAATATAAGAGC-3', PTENR 5'-TCCCTTATCAGATACATGACTTTCA-3' [32].

KRASF 5'-CGATACACGTCTGCAGTCAAC-3', KRASR 5'-ACCCTGACATACTCCCAAGGA-3' [30].

HRASF 5'-TCTAGAGGAAGCAGGAGACAGG-3', HRASR 5'-CTTTTCCCATCACTGGGTCAT-3' [33].

Statistics details for in silico analyses

For Gene Ontology (GO) and Kyoto Encyclopedia of Genes and Genomes (KEGG) enrichment

analysis, we used Fisher's Exact test for computing statistical difference [34, 35]. Correlational analyses were carried out using the Pearson method. For comparisons, a student t-test was adopted in the current study. All the analyses were carried out in R version 3.6.3 software.

Results

Ferroptosis driver gene acquisition, PPI network construction, module, and hub genes discovery

In total 233 ferroptosis driver genes were downloaded from the ferrDB database, which underwent analysis using STRING to determine their PPI. A total of 233 nodes and 1567 edges were identified in the constructed PPI network (**Figure 1A**). MCODE plugin was then applied on this network to identify the top module. The identified top module consisted of 27 nodes (highlighted in yellow) (**Figure 1B**, **1C**). Lastly, Cytohubba analysis further revealed top four hub genes in this module, namely TP53 (tumor protein 53), PTEN (Phosphatase and TENsin homolog deleted on chromosome 10), KRAS (Ki-ras2 Kirsten rat sarcoma viral oncogene homolog), and HRAS (Harvey Rat sarcoma virus), based on their degree score method (**Figure 1D**).

Expression paradigm of the hub genes in TCGA

The ULACAN database was utilized to evaluate the expression profiles of key hub genes including TP53, PTEN, KRAS, and HRAS in the HNSC TCGA dataset. The findings showed that mRNA and protein expression levels of these genes were significantly higher ($P < 0.05$) in HNSC samples compared to non-tumor tissue samples, as demonstrated in **Figure 1E-G**. Further analysis using the UALCAN, also revealed that TP53, PTEN, KRAS, and HRAS hub genes were up-regulated in HNSC samples with various clinical findings at both mRNA and protein levels when compared to normal control samples (**Figures 2** and **3**).

Expression verification and survival analysis

The expression profiles of key hub genes including TP53, PTEN, KRAS, and HRAS were further verified in additional GEPIA, OncoDB, and MuTarget TCGA HNSC cohorts. Results of the verification analysis indicated significant up-regulation of these genes in HNSC samples compared to controls (**Figure 4A-C**). Additionally, survival outcome analysis showed that the up-regulation of TP53, PTEN, KRAS, and HRAS key hub genes were linked to worse prognosis in HNSC patients (**Figure 4D**). These findings suggest that dysregulation of TP53, PTEN, KRAS, and HRAS key hub genes may be a significant factor for the development and prognosis of HNSC.

Sub-cellular localization and protein expression validation analysis

The HPA database analysis indicated that the TP53 protein was predominantly located in the nucleoplasm, vesicles, and cytosol, while the PTEN protein was present in both the cytosol and nucleoplasm. Moreover, the HRAS protein was observed in the cytosol and focal adhesion sites, with HRAS being identified in the cytosol and nucleosome as well (**Figure 5A**). **Figure 5B** shows the examination of TP53, PTEN, KRAS, and HRAS genes using IHC-based expression data from HPA. It was revealed that the protein levels of TP53, PTEN, KRAS, and HRAS were higher in HNSC tissues compared to normal samples. Therefore, it can be concluded that up-regulation of TP53, PTEN, KRAS, and HRAS proteins occurred in HNSC relative to control samples (**Figure 5B**).

Development of hub gene-based prognostic model

In the TP53, PTEN, KRAS, and HRAS gene-based prognostic model analysis, the TCGA-HNSC dataset was used a training dataset while GSE75538, GSE65858, and E_MTAB_8588 datasets were used as validation datasets. We constructed a stepwise Cox regression model including the parameters of hazard ratio, c-index, and risk score. The evaluation of the predictive prognostic model using a c-index revealed the efficacy and robustness of the model for prediction of the prognosis of HNSC patients (**Figure 5C**).

Genetic alterations and their effect on the survival of HNSC patients

Through analysis of key hub genes TP53, PTEN, KRAS, and HRAS using the cBioPortal web-source, it was found that mutations in the TP53

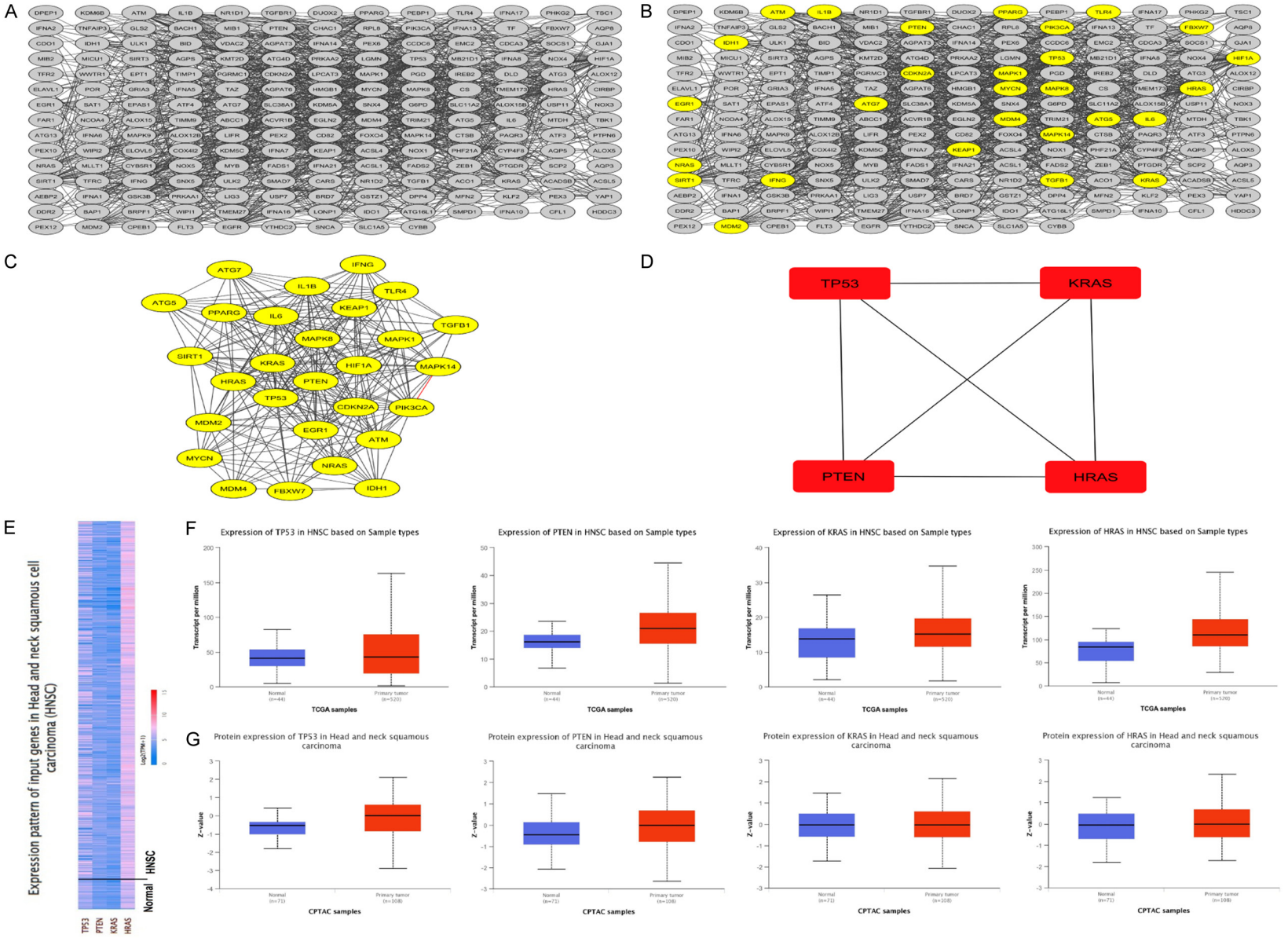
A
B
C
D
E
F
G
TP53
KRAS
PTEN
HRAS
Expression pattern of input genes in Head and neck squamous cell carcinoma (HNSC)
Normal
HNSC
Expression of TP53 in HNSC based on Sample types
Expression of PTEN in HNSC based on Sample types
Expression of KRAS in HNSC based on Sample types
Expression of HRAS in HNSC based on Sample types
Transcript per million
TCGA samples
Protein expression of TP53 in Head and neck squamous carcinoma
Protein expression of PTEN in Head and neck squamous carcinoma
Protein expression of KRAS in Head and neck squamous carcinoma
Protein expression of HRAS in Head and neck squamous carcinoma
Z-value
CPTAC samples

Figure 1. A PPI network of the ferroptosis driver genes, a significant module in the constructed PPI network, a PPI network of the identified hub genes, and mRNA and protein expression profiling of hub genes. (A) A PPI network of the ferroptosis-related genes, (B, C) A PPI network of the most significant module, (D) A PPI network of identified four hub genes, (E) A heatmap of TP53, PTEN, KRAS, and HRAS hub genes in HNSC sample group and normal control group, (F) Box plot presentation of TP53, PTEN, KRAS, and HRAS hub genes mRNA expression in HNSC sample group and normal control group, (G) Box plot presentation of TP53, PTEN, KRAS, and HRAS hub genes protein expression in HNSC sample group and normal control group. HNSC, Head and neck squamous cell carcinoma; TP53, tumor protein 53; PTEN, Phosphatase and TENsin homolog deleted on chromosome 10; KRAS, Ki-ras2 Kirsten rat sarcoma viral oncogene homolog; HRAS, Harvey Rat sarcoma virus; mRNA, messenger RNA.

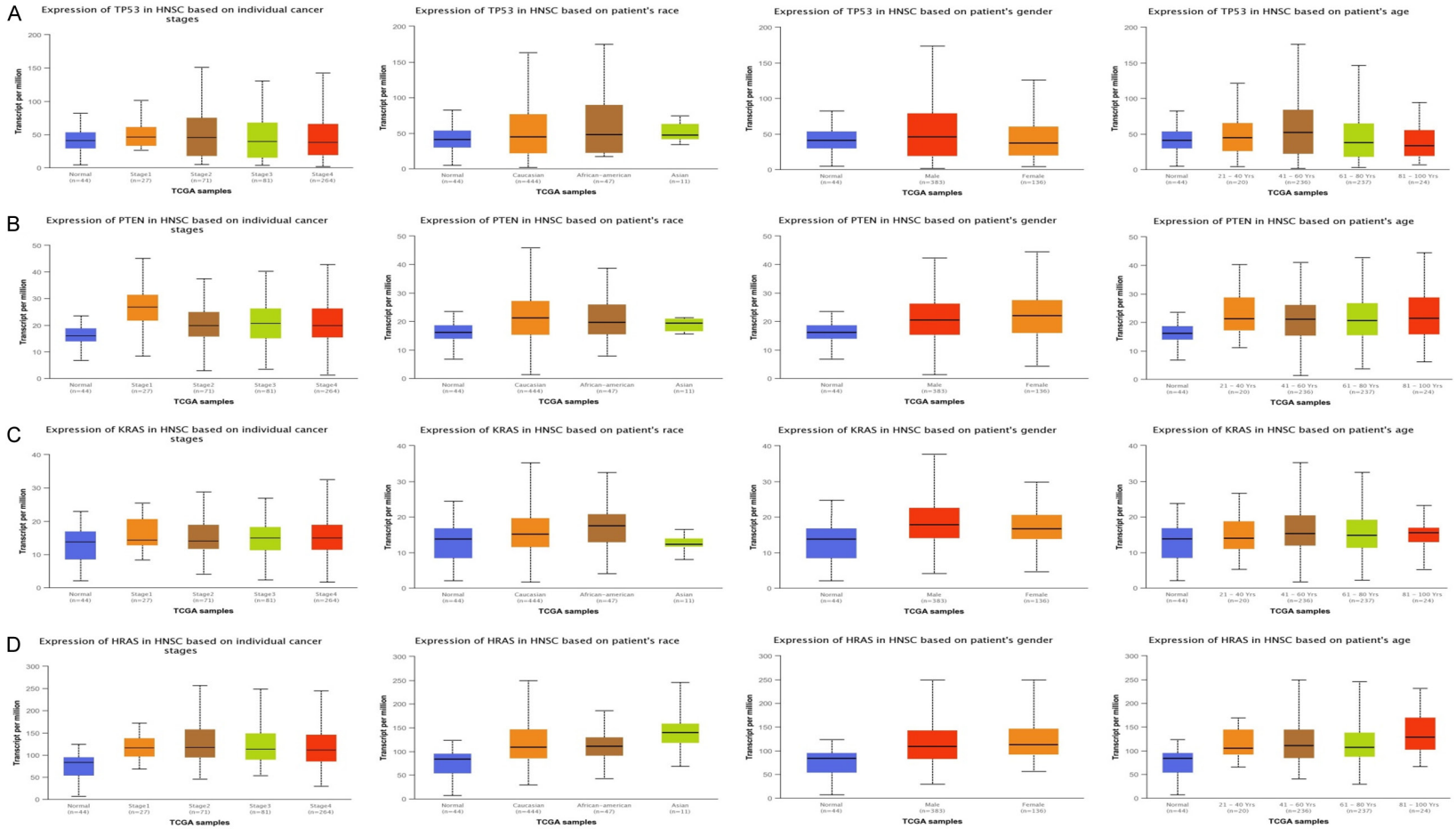

Figure 2. mRNA expression profiling of TP53, PTEN, KRAS, and HRAS in HNSC samples of different clinical variables relative to controls by UALCAN. (A) mRNA expression profiling of TP53 in HNSC samples of different clinical variables, (B) mRNA expression profiling of PTEN in HNSC samples of different clinical variables, (C) mRNA expression profiling of KRAS in HNSC samples of different clinical variables, (D) mRNA expression profiling of HRAS in HNSC samples of different clinical variables. HNSC, Head and neck squamous cell carcinoma; TP53, tumor protein 53; PTEN, Phosphatase and TENsin homolog deleted on chromosome 10; KRAS, Ki-ras2 Kirsten rat sarcoma viral oncogene homolog; HRAS, Harvey Rat sarcoma virus.

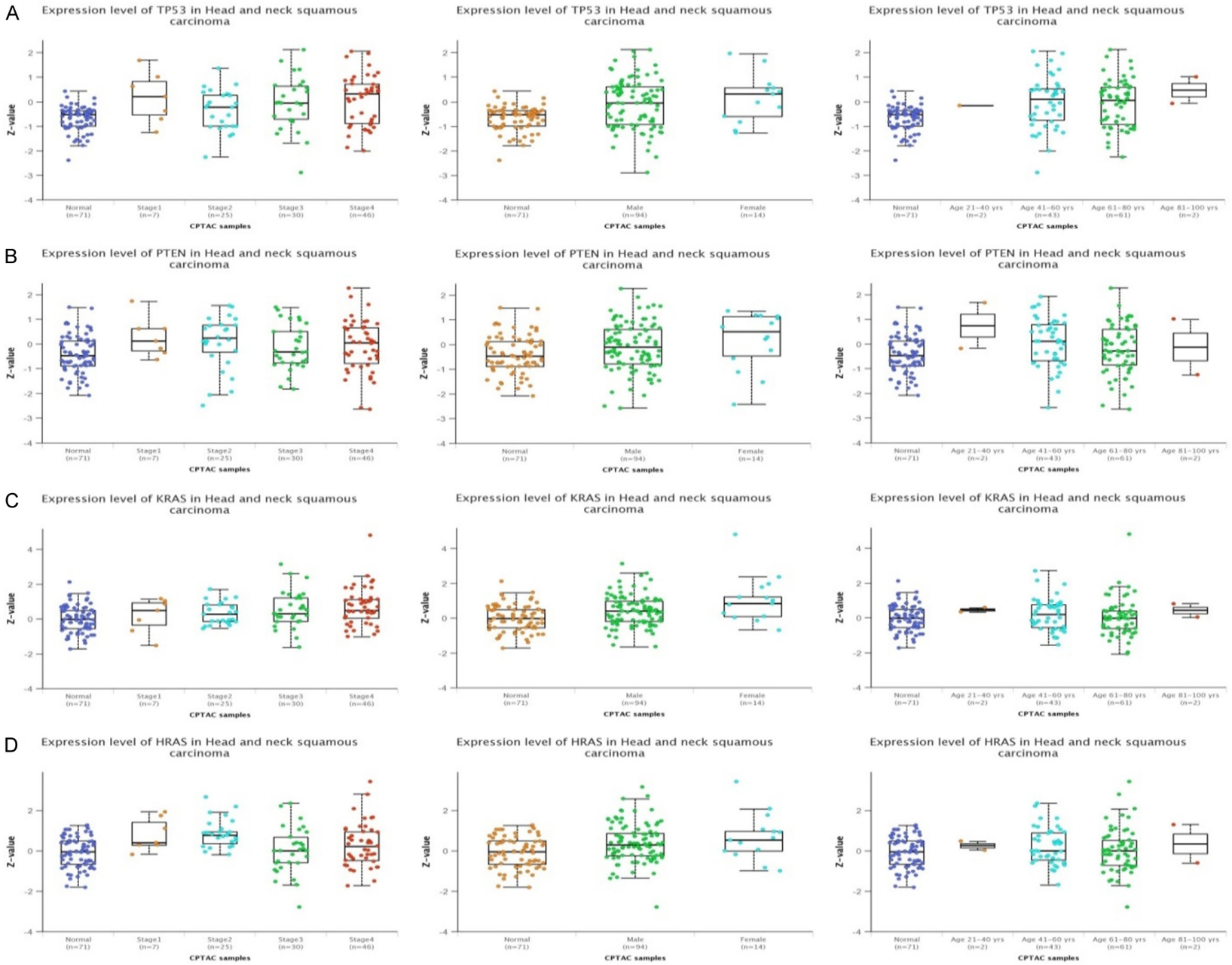
A
Expression level of TP53 in Head and neck squamous carcinoma
Z-value
Normal (n=71)
Stage1 (n=7)
Stage2 (n=25)
Stage3 (n=30)
Stage4 (n=46)
CPTAC samples
Expression level of TP53 in Head and neck squamous carcinoma
Z-value
Normal (n=71)
Male (n=94)
Female (n=14)
CPTAC samples
Expression level of TP53 in Head and neck squamous carcinoma
Z-value
Normal (n=71)
Age 21-40 yrs (n=2)
Age 41-60 yrs (n=43)
Age 61-80 yrs (n=61)
Age 81-100 yrs (n=2)
CPTAC samples
B
Expression level of PTEN in Head and neck squamous carcinoma
Z-value
Normal (n=71)
Stage1 (n=7)
Stage2 (n=25)
Stage3 (n=30)
Stage4 (n=46)
CPTAC samples
Expression level of PTEN in Head and neck squamous carcinoma
Z-value
Normal (n=71)
Male (n=94)
Female (n=14)
CPTAC samples
Expression level of PTEN in Head and neck squamous carcinoma
Z-value
Normal (n=71)
Age 21-40 yrs (n=2)
Age 41-60 yrs (n=43)
Age 61-80 yrs (n=61)
Age 81-100 yrs (n=2)
CPTAC samples
C
Expression level of KRAS in Head and neck squamous carcinoma
Z-value
Normal (n=71)
Stage1 (n=7)
Stage2 (n=25)
Stage3 (n=30)
Stage4 (n=46)
CPTAC samples
Expression level of KRAS in Head and neck squamous carcinoma
Z-value
Normal (n=71)
Male (n=94)
Female (n=14)
CPTAC samples
Expression level of KRAS in Head and neck squamous carcinoma
Z-value
Normal (n=71)
Age 21-40 yrs (n=2)
Age 41-60 yrs (n=43)
Age 61-80 yrs (n=61)
Age 81-100 yrs (n=2)
CPTAC samples
D
Expression level of HRAS in Head and neck squamous carcinoma
Z-value
Normal (n=71)
Stage1 (n=7)
Stage2 (n=25)
Stage3 (n=30)
Stage4 (n=46)
CPTAC samples
Expression level of HRAS in Head and neck squamous carcinoma
Z-value
Normal (n=71)
Male (n=94)
Female (n=14)
CPTAC samples
Expression level of HRAS in Head and neck squamous carcinoma
Z-value
Normal (n=71)
Age 21-40 yrs (n=2)
Age 41-60 yrs (n=43)
Age 61-80 yrs (n=61)
Age 81-100 yrs (n=2)
CPTAC samples

Figure 3. Protein expression profiling of TP53, PTEN, KRAS, and HRAS in HNSC samples of different clinical variables relative to controls via UALCAN. (A) Protein expression profiling of TP53 in HNSC samples of different clinical variables, (B) Protein expression profiling of PTEN in HNSC samples of different clinical variables, (C) Protein expression profiling of KRAS in HNSC samples of different clinical variables, and (D) Protein expression profiling of HRAS in HNSC samples of different clinical variables. HNSC, Head and neck squamous cell carcinoma; TP53, tumor protein 53; PTEN, Phosphatase and TENsin homolog deleted on chromosome 10; KRAS, Ki-ras2 Kirsten rat sarcoma viral oncogene homolog; HRAS, Harvey Rat sarcoma virus.

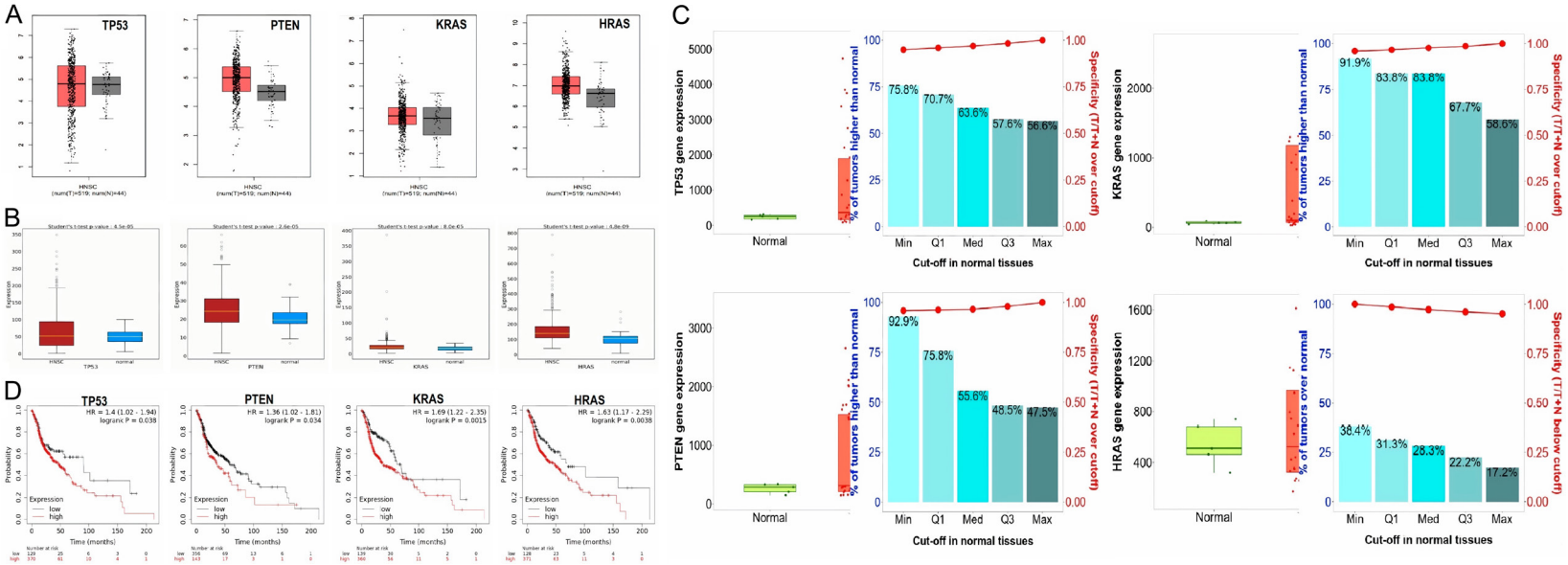

Figure 4. Expression validation and survival analysis of TP53, PTEN, KRAS, and HRAS. (A) Expression validation of TP53, PTEN, KRAS, and HRAS in HNSC and normal samples from GEPIA database, (B) Expression validation of TP53, PTEN, KRAS, and HRAS in HNSC and normal samples from OncoDB database, (C) Expression validation of TP53, PTEN, KRAS, and HRAS in HNSC and normal samples via MuTarget database, and (D) Survival analysis of TP53, PTEN, KRAS, and HRAS in HNSC and normal samples from the GEPIA database. HNSC, Head and neck squamous cell carcinoma; TP53, tumor protein 53; PTEN, Phosphatase and TENsin homolog deleted on chromosome 10; KRAS, Ki-ras2 Kirsten rat sarcoma viral oncogene homolog; HRAS, Harvey Rat sarcoma virus.

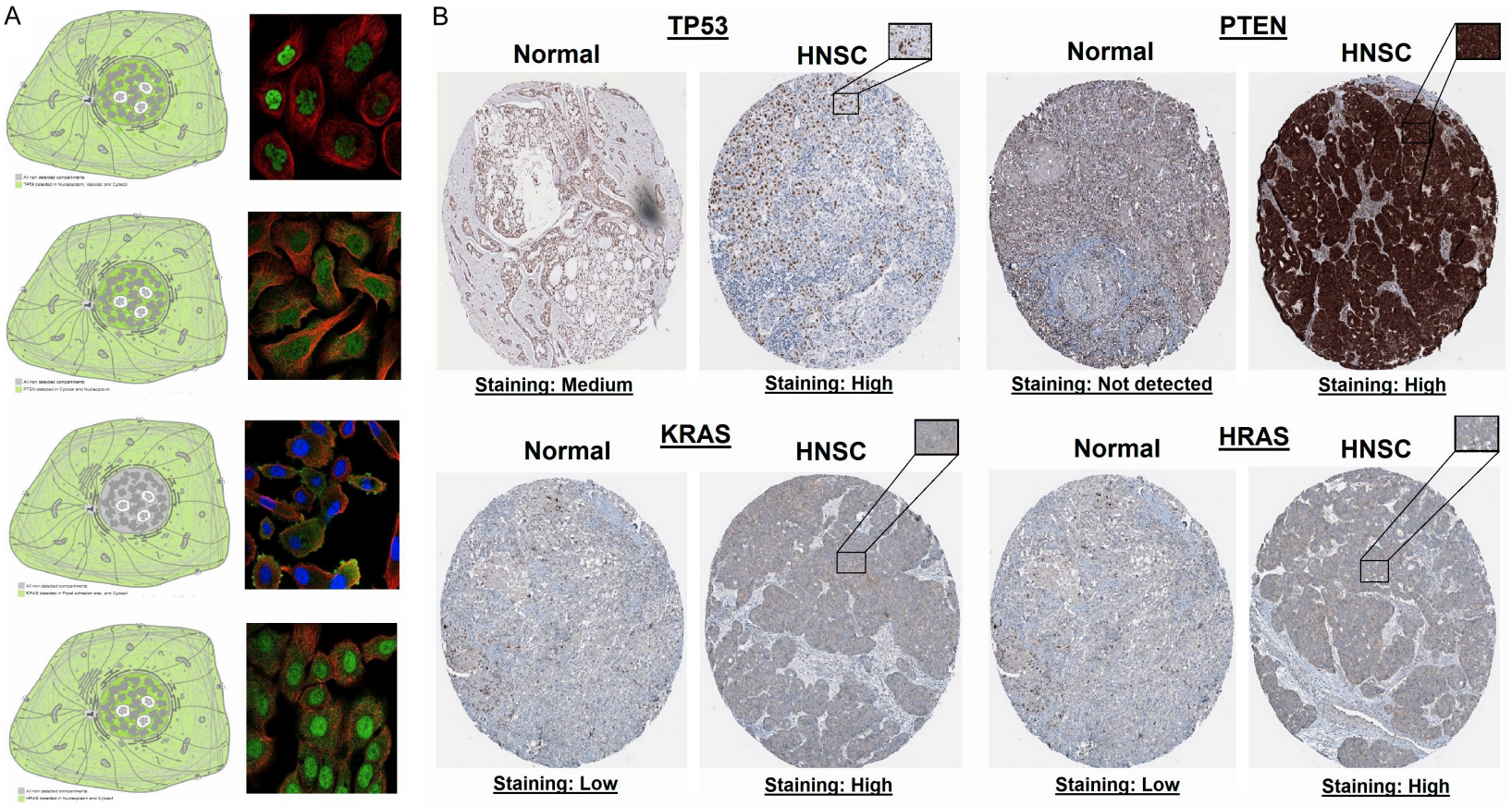
A
B
TP53
Normal
HNSC
Staining: Medium
Staining: High
PTEN
Normal
HNSC
Staining: Not detected
Staining: High
KRAS
Normal
HNSC
Staining: Low
Staining: High
HRAS
Normal
HNSC
Staining: Low
Staining: High

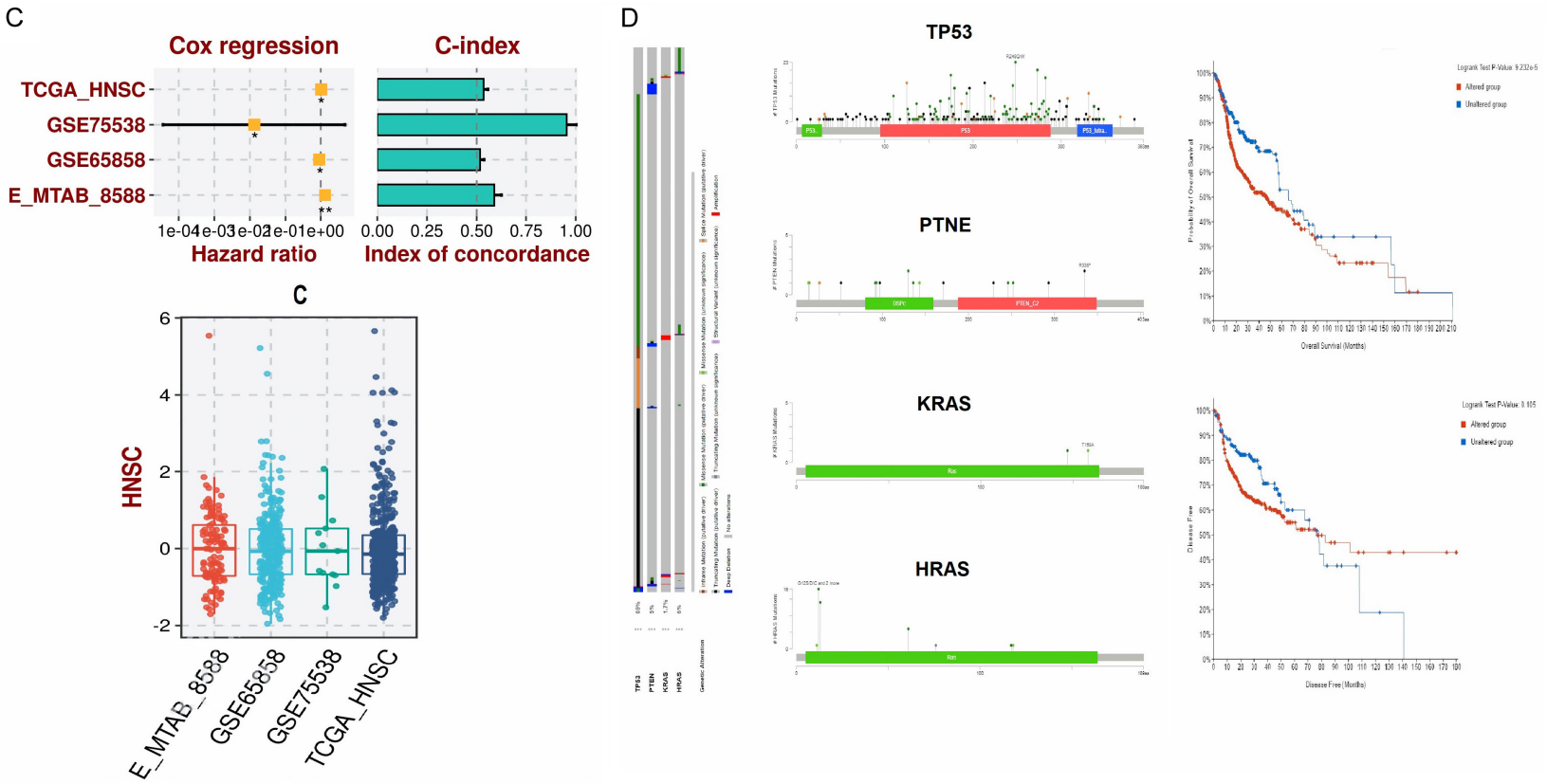

Figure 5. Subcellular localization and protein expression validation, construction of prognostic model, exploration of genetic alteration frequencies, OS, and DFS analyses of hub genes. (A) Subcellular localization prediction of TP53, PTEN, KRAS, and HRAS, and (B) Protein expression analysis of TP53, PTEN, KRAS, and HRAS in HNSC and normal samples, (C) Univariate Cox regression analysis, c-index scores, and risk scores and (D) Types, frequencies, and location of the genetic alterations, OS and DFS analysis of TP53, PTEN, KRAS, and HRAS in genetically altered and unaltered HNSC groups. HNSC, Head and neck squamous cell carcinoma; TP53, tumor protein 53; PTEN, Phosphatase and TENsin homolog deleted on chromosome 10; KRAS, Ki-ras2 Kirsten rat sarcoma viral oncogene homolog; HRAS, Harvey Rat sarcoma virus; OS, Overall Survival; DFS, Disease free survival.

gene were present in 39% of HNSC samples. Additionally, mutations in the PTEN, KRAS, and HRAS genes were present in 5%, 1.7%, and 6% of HNSC samples, respectively (**Figure 5D**). The most common genetic variations observed in TP53 and HRAS were missense mutations (**Figure 5D**), while PTEN and KRAS were most frequently affected by deep amplification and deep deletion genetic variations, respectively. Furthermore, examining the HNSC samples that had genetic alterations in the TP53, PTEN, KRAS, and HRAS hub genes versus those without such alterations using OS and DFS analyses revealed that the former exhibited poorer OS and DFS outcomes compared to the latter group (**Figure 5D**).

Methylome analysis of the TP53, PTEN, KRAS, and HRAS

The methylation levels of TP53, PTEN, KRAS, and HRAS genes, which are key hub genes in HNSC tumorigenesis, were further examined to delve deeper into their oncogenic roles. MEXPRESS and OncoDB databases were utilized for this purpose. It was observed through MEXPRESS analysis in **Figure 6A** that HNSC tissue samples had lower methylation levels of these genes compared to normal tissue. OncoDB analysis also confirmed this finding and its results are illustrated in **Figure 6B**.

Gene enrichment analysis

Next, we performed GO and KEGG enrichment analyses. Among GO terms, hub genes were enriched in "Beta-catenin destruction complex, Wnt signalosome, extrinsic component of plasma membrane, and chromosomal region" etc., CC terms, "GMP binding, DNA-dependent protein kinase activity, Histone deacetylase regulator activity, and LRR domain binding" etc., MF terms, "Replicative senescence, determination of adult lifespan, response to X-Ray, and multicellular organism aging" etc., BP terms, and "Endometrial cancer, thyroid cancer, bladder cancer, and melanoma" etc., and KEGG terms (**Figure 7A-D**).

Immune cell infiltration analysis

Across the HNSC TCGA cohort, the TIMER database was used to evaluate correlations among CD8+ T cells, CD4+ T cells, and macrophage infiltration level and expression and expressions of the TP53, PTEN, KRAS, and HRAS hub genes. According to the outcomes of the TIMER analysis, higher expressions of TP53, PTEN, KRAS, and HRAS were correlated with higher levels of CD8+ T cells, CD4+ T cells, and macrophages (**Figure 7E**).

miRNA network of TP53, PTEN, KRAS, and HRAS

We used ENCORI and Cytoscape to create miRNA-mRNA co-regulatory networks for TP53, PTEN, KRAS, and HRAS. These networks contained a total of 470 miRNAs and 4 mRNAs (**Figure 8**). By analyzing the networks, we discovered that the miRNA has-let-7a-5p targets all of the hub genes simultaneously. Consequently, we speculate that has-let-7a-5p, together with TP53, PTEN, KRAS, and HRAS (**Figure 8**), may play a significant role in inducing HNSC.

Drug prediction analysis of the hub genes

Through the DrugBank database, we selected a total of 12 drugs (**Table 1**) which may influence TP53, PTEN, KRAS, and HRAS hub gene expression, including some well known drugs, namely cisplatin, fluorouracil, and estradiol (**Table 1**). The identified drugs in this work may be utilized in the treatment of HNSC patients.

RNA-seq, RT-qPCR, and targeted bisulfite-seq analyses-based validation of the hub gene expression and methylation levels

In the current study, using RNA-seq, RT-qPCR, and targeted bisulfite-seq data of one HNSC (FaDu) and one normal human oral keratinocyte (HOK) cell line, the expression and promoter methylation levels of identified four hub genes were validated. As shown in **Figure 9A**, it was noted by RNA-seq analysis that the TP53, PTEN, KRAS, and HRAS hub genes were expressed in both HNSC and normal control cell lines and FPKM values of the TP53, PTEN, KRAS, and HRAS were higher in the HNSC cell line (FaDu) as compared to normal cell line (HOK) (**Figure 9A**).

To further validate the aforementioned bioinformatic analysis, the mRNA expression levels of these hub genes were obtained by the RT-qPCR experiment in HNSC cell line (FaDu) pairs of normal control cell line (HOK). As suggested in

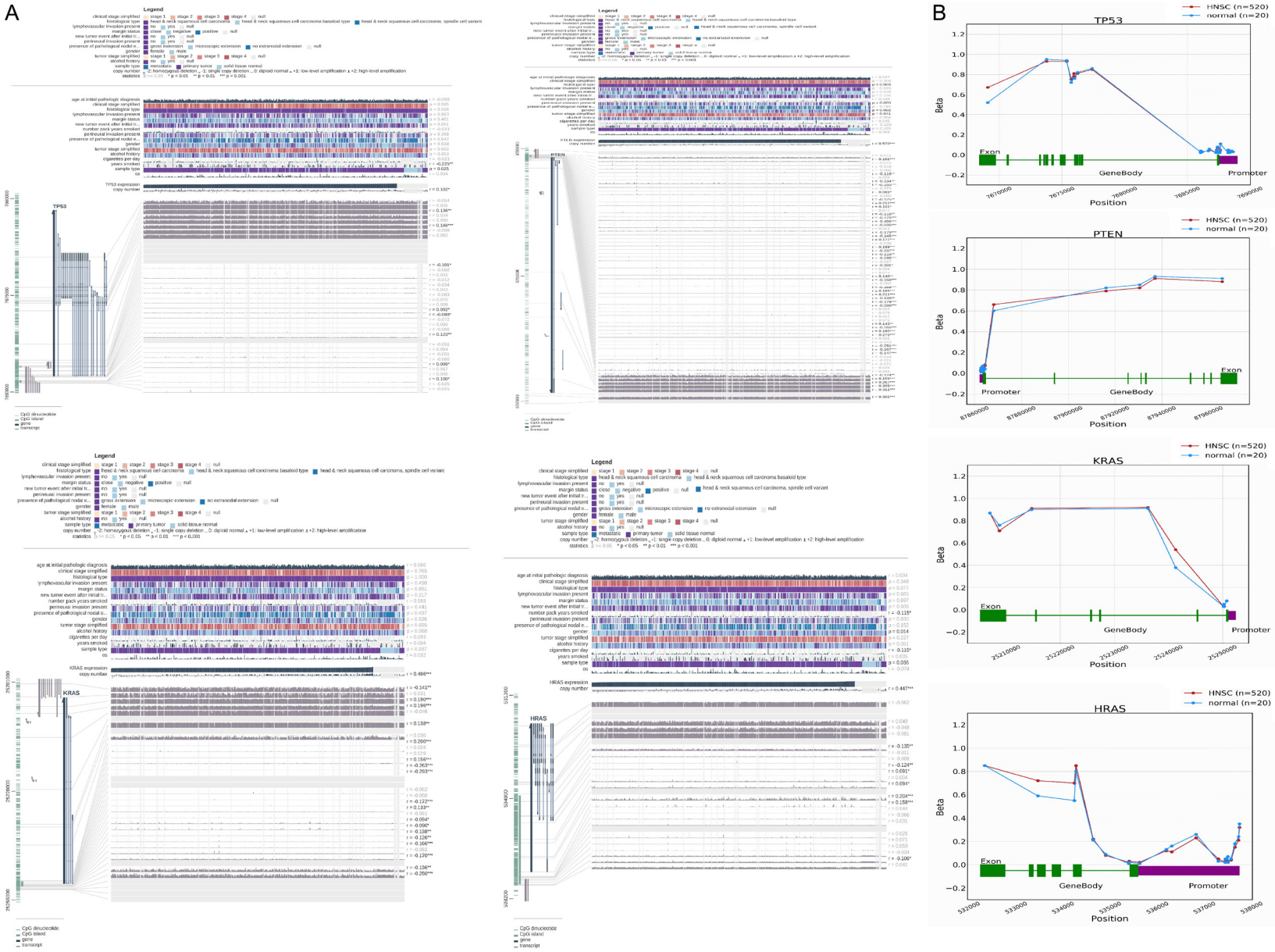
A
B
HNSC (n=520)
normal (n=20)
TP53
PTEN
KRAS
HRAS
Beta
Position
Exon
GeneBody
Promoter

Figure 6. Methylation status exploration of TP53, PTEN, KRAS, and HRAS through MEXPRESS and OncoDB in HNSC and normal samples. (A) Methylation status exploration of TP53, PTEN, KRAS, and HRAS through MEXPRESS, and (B) Methylation status exploration of TP53, PTEN, KRAS, and HRAS from OncoDB. HNSC, Head and neck squamous cell carcinoma; TP53, tumor protein 53; PTEN, Phosphatase and TENsin homolog deleted on chromosome 10; KRAS, Ki-ras2 Kirsten rat sarcoma viral oncogene homolog; HRAS, Harvey Rat sarcoma virus.

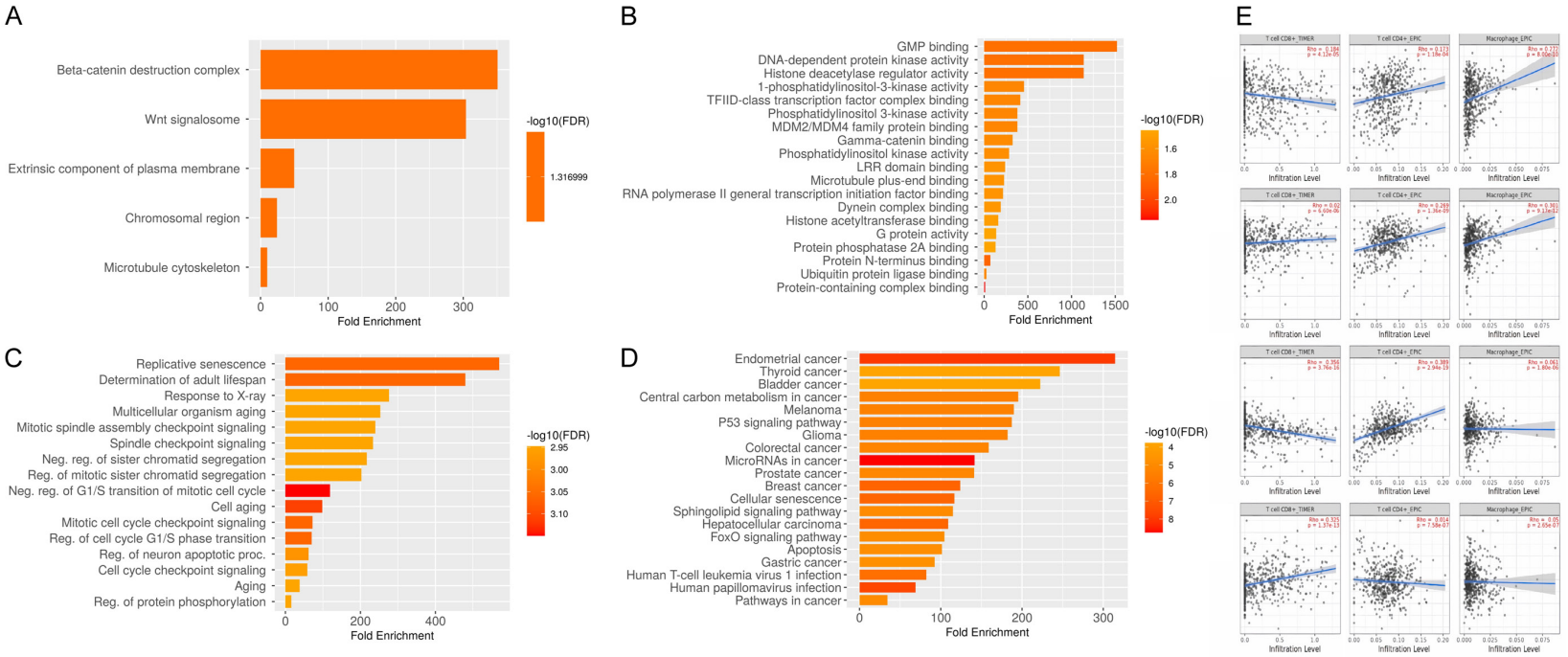

Figure 7. Gene enrichment and immune cell infiltration analyses of TP53, PTEN, KRAS, and HRAS. (A) TP53, PTEN, KRAS, and HRAS associated CC terms, (B) TP53, PTEN, KRAS, and HRAS associated MF terms, (C) TP53, PTEN, KRAS, and HRAS associated BP terms, (D) TP53, PTEN, KRAS, and HRAS associated KEGG terms, and (E) Correlation of TP53, PTEN, KRAS, and HRAS hub genes expression with different immune cells (CD8+ T, CD4+ T, and Macrophages) infiltration level. TP53, tumor protein 53; PTEN, Phosphatase and TENsin homolog deleted on chromosome 10; KRAS, Ki-ras2 Kirsten rat sarcoma viral oncogene homolog; HRAS, Harvey Rat sarcoma virus; CC, Cellular component; MF, Molecular function; BP, Biological processes; KEGG, Kyoto Encyclopedia of Genes and Genomes.

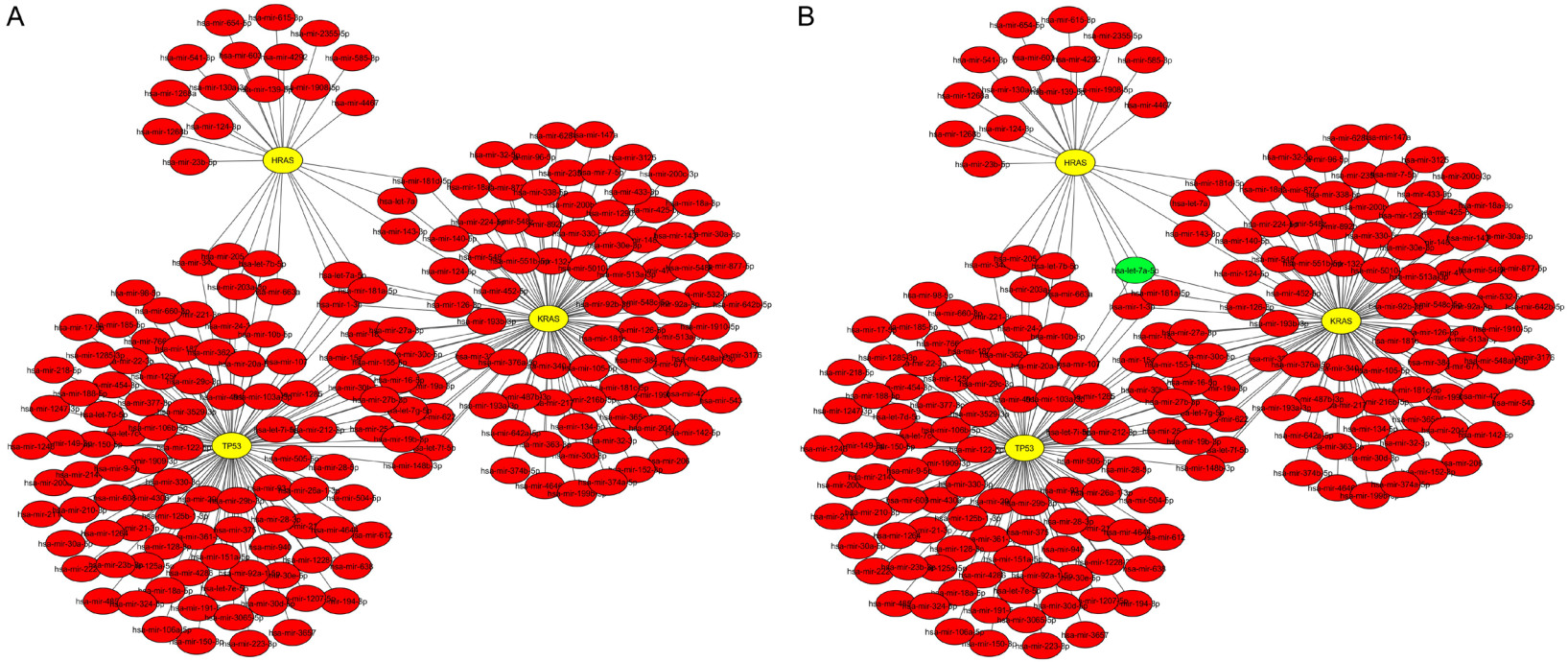

Figure 8. miRNA-mRNA co-regulatory network of TP53, PTEN, KRAS, and HRAS hub genes. (A) A PPI of miRNAs targeting hub genes, and (B) A PPI highlighting most important miRNA (hsa-let-7a-5p) targeting all hub genes. Red color nodes: miRNAs, yellow color nodes: mRNAs, and green color node: hsa-let-7a-5p.

Table 1. DrugBank-based hub gene-associated drugs

Sr. No	Hub gene	Drug name	Effect	Reference	Group
1	TP53	Acetaminophen	Decrease expression of TP53 mRNA	A20420	Approved
		Doxorubicin		A22419	
2	PTEN	Estradiol	Decrease expression of PTEN mRNA	A21359	Approved
		Cisplatin		A22257	
		Fluorouracil		A22637	
		Resveratrol		A23878	
3	KRAS	Estradiol	Decrease expression of KRAS mRNA	A21098	Approved
		Estradiol		A21100	
		Methotrexate		A23222	
4	HRAS	Cyclosporine	Decrease expression of HRAS mRNA	A20661	Approved
		Decitabine		A21197	
		Quercetin		A23791	

TP53, tumor protein 53; PTEN, Phosphatase and TENsin homolog deleted on chromosome 10; KRAS, Ki-ras2 Kirsten rat sarcoma viral oncogene homolog; HRAS, Harvey Rat sarcoma virus; mRNA, Messenger RNA.

Figure 9B, there were notable differences between FaDu cell line and HOK cell line in all four hub genes, including TP53, PTEN, KRAS, and HRAS (**Figure 9B**). Interestingly, all these genes had up-regulation in HNSC cell line relative to normal control cell line (HOK) (**Figure 9B**) as previously predicted by TCGA datasets and analyzed by RNA-seq technique Moreover, the obtained beta values of the TP53, PTEN, KRAS, and HRAS via targeted bisulfite-seq analysis were lower in the HNSC cell line (FaDu) as compared to the normal cell line (HOK) (**Figure 9C**).

RT-qPCR validation analysis of TP53, PTEN, KRAS, and HRAS

To further validate the aforementioned bioinformatic analysis, the mRNA expression levels of these hub genes (TP53, PTEN, KRAS, and HRAS) were obtained by the RT-qPCR experiment in HNSC cell line (FaDu) pairs of normal control cell line (HOK). As suggested in **Figure 9**, there were differences between FaDu cell line and HOK cell line in all four hub genes, including TP53, PTEN, KRAS, and HRAS (**Figure 9**). Interestingly, all these genes had up-regulation in the HNSC cell line relative to normal control cell line (HOK) (**Figure 9**) as previously predicted by TCGA datasets and analyzed by RNA-seq technique.

Discussion

Given the rising incidence of HNSC globally, there is a need for reliable molecular biomarkers, since HNSC is a heterogeneous disease [36]. Ferroptosis, a novel form of programmed cell death, plays a multifaceted role in tumor development [37]. However, research on ferroptosis in HNSC is currently limited [38]. Accordingly, exploring ferroptosis influencer genes linked to HNSC progression and prognosis is both critical and compelling. Focusing on 233 ferroptosis driver genes, an exploration of HNSC-associated hub genes was carried out in this study using a range of in vitro and in vivo methods. As a result, it was found that TP53, PTEN, KRAS, and HRAS were up-regulated hub genes, serving as possible diagnostic and prognostic biomarkers for HNSC patients. Genetic mutations and promoter hypomethylation were also examined as causative factors behind the up-regulation of these genes in HNSC.

TP53 is a tumor suppressor gene that is frequently mutated in various types of cancer [39]. Its primary function is to maintain genomic stability and prevent the formation of cancerous cells by inducing cell cycle arrest, DNA repair, or apoptosis (programmed cell death) in response to DNA damage or other stresses [40]. Recent studies suggest that TP53 may also play a role in regulating ferroptosis, a form of regulated cell death triggered by iron-dependent lipid peroxidation [41]. Ferroptosis is a novel mechanism of cell death that has been implicated in various physiological and pathological conditions, including cancer [42]. In cancer cells, the dysregulation of iron metabolism and lipid peroxidation can promote tumor growth and metastasis by suppressing ferrop-

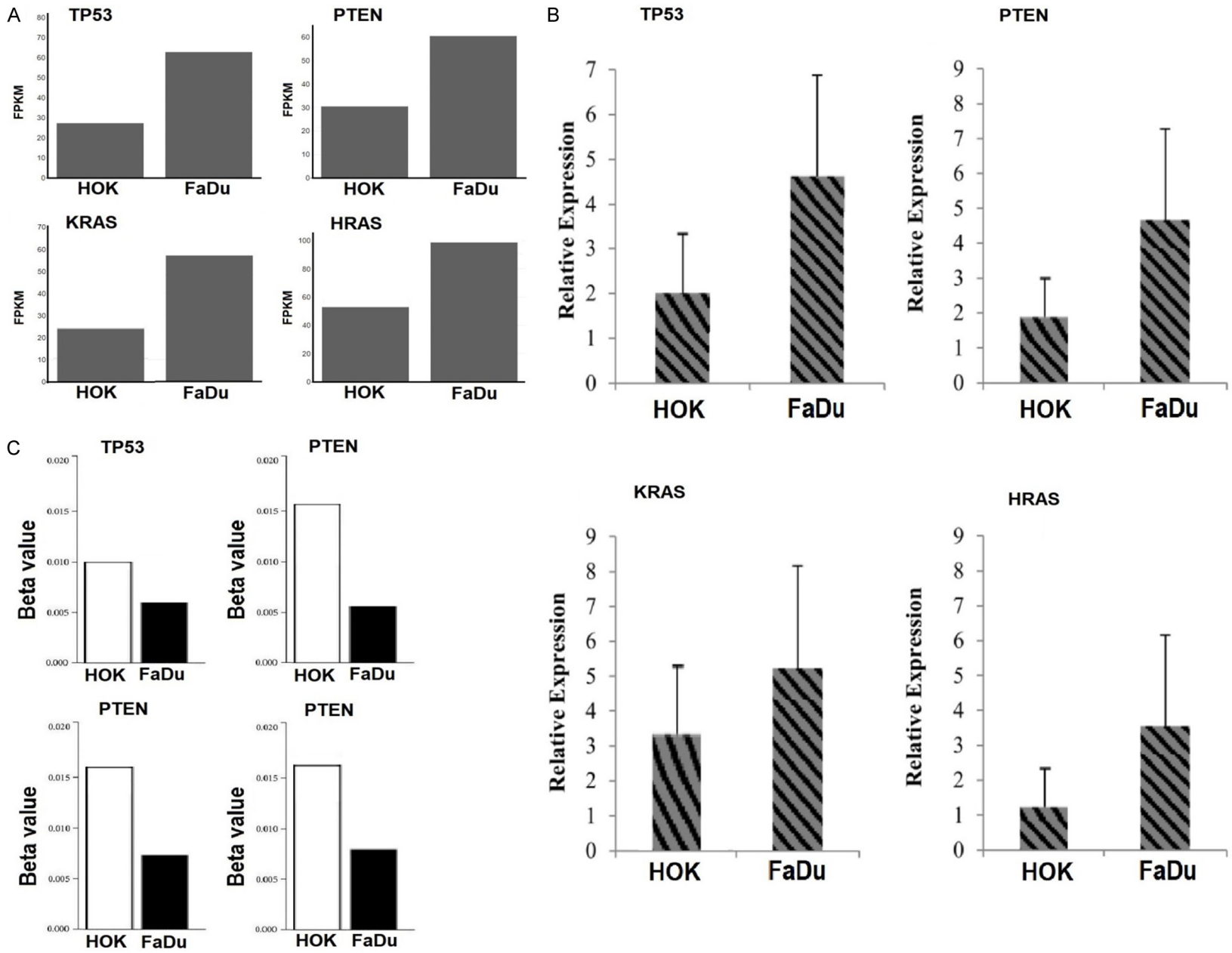
A
TP53
PTEN
KRAS
HRAS
FPKM
HOK
FaDu
B
TP53
PTEN
KRAS
HRAS
Relative Expression
HOK
FaDu
C
TP53
PTEN
PTEN
PTEN
Beta value
HOK
FaDu

Figure 9. Validating TP53, PTEN, KRAS, and HRAS expressions and promoter methylation levels using HNSC (FaDu), and the normal control cell line (HOK) through RNA-seq and targeted bisulfite-seq analysis. (A) RNA-seq based expression validation of TP53, PTEN, KRAS, and HRAS, (B) RT-qPCR based expression validation of TP53, PTEN, KRAS, and HRAS and (C) Beta values based promoter methylation based validation of TP53, PTEN, KRAS, and HRAS. TP53, tumor protein 53; PTEN, Phosphatase and TENsin homolog deleted on chromosome 10; KRAS, Ki-ras2 Kirsten rat sarcoma viral oncogene homolog; HRAS, Harvey Rat sarcoma virus; RNA-seq, RNA-sequencing; RT-qPCR, Reverse Transcription Quantitative Real-Time Polymerase Chain Reaction; bisulfite-seq, bisulfite-sequencing.

tosis [43]. Several studies have shown that TP53 mutations and dysregulation can affect the sensitivity of cancer cells to ferroptosis-inducing agents, either by impairing the expression or activity of ferroptosis regulators, such as p21, SLC7A11, or GPX4 or by promoting the up-regulation of anti-ferroptotic genes, such as BCL-xL or MDM2 [44, 45]. TP53 up-regulation has been found to resist ferroptosis in various cancer types including, colorectal cancer, non-small cell lung cancer, pancreatic cancer, breast cancer, ovarian cancer, and glioblastoma [9, 46].

PTEN gene, which stands for phosphatase and TENsin homolog deleted on chromosome 10, is a tumor suppressor gene that plays a critical role in the control of cell growth, proliferation, and survival [47]. Recent research has shown that PTEN plays a key role in regulating the sensitivity of cancer cells to ferroptosis [48]. According to earlier research, it was observed that cancer cells with loss of PTEN function are resistant to ferroptosis, and that PTEN is required for the activation of ferroptosis in response to certain drugs and other stressors [49]. In addition, PTEN has been shown to regulate the expression of various genes involved in ferroptosis, including those involved in lipid metabolism, iron handling, and redox regulation [50]. The identification of PTEN as a ferroptosis-resistant biomarker in cancer holds significant implications for the development of new cancer treatments [50]. Targeting the PTEN pathway may enhance the efficacy of ferroptosis-inducing agents in the treatment of cancer [49]. This approach may also provide a means to overcome resistance to other forms of cell death, such as apoptosis and necroptosis. PTEN dysregulation is related to ferroptosis resistance in various cancers, including prostate cancer, glioblastoma, hepatocellular carcinoma, melanoma, pancreatic cancer, and lung cancer [51, 52].

The KRAS gene plays a crucial role in regulating cell growth and division [53]. It instructs the body to produce a protein that is involved in transmitting signals within cells, which are essential for cell division [53]. The KRAS gene has been identified as a ferroptosis-resistant biomarker in cancer [54]. This gene is frequently mutated and dysregulated in cancer, and recent studies have shown that it can facilitate ferroptosis resistance by promoting lipid biosynthesis and antioxidant response [55, 56]. Targeting KRAS-induced ferroptosis resistance may be a viable strategy for cancer therapy [55]. KRAS dysregulation has been associated with ferroptosis resistance in several types of cancer, including lung cancer, pancreatic cancer, colorectal cancer, and ovarian cancer [57, 58]. Overall, less research has been done so far on exploring ferroptosis resistant role of HRAS in human cancers.

HRAS encodes a small GTPase that belongs to the Ras oncogene family [59]. HRAS is frequently mutated and dysregulated in human cancers, particularly in HNSC cell carcinoma, bladder cancer, and melanoma [60]. Recent studies have shown that HRAS mutations or overexpression induce ferroptosis resistance in cancer cells [61, 62]. HRAS-mediated ferroptosis is dependent on the production of reactive oxygen species (ROS) and the modulation of glutathione peroxidase 4 (GPX4) activity [8]. Moreover, transcriptomic analysis has demonstrated that HRAS expression is positively associated with ferroptosis-related genes, such as ACSL4, SLC7A11, and DPP4 [63]. In addition, HRAS expression correlates with low levels of antioxidants and high levels of lipid peroxidation products, which are hallmarks of ferroptosis [64]. These findings suggest that HRAS might serve as a useful biomarker for ferroptosis in cancer.

Numerous research studies have recently asserted that immune cell infiltration may greatly hasten the progression of cancer [65]. For instance, according to Hu et al., an increased expression of the OGN gene can stimulate infiltration of CD8+ T immune cells,

resulting in the inhibition of blood vessel formation in cases of colon cancer [66]. With this critical information in mind, we examined the connections between hub genes and significant immune cell infiltrates. Notably, greater expressions of TP53, PTEN, KRAS, and HRAS showed a positive correlation with the presence of CD8+ T cells, CD4+ T cells, and macrophages in HNSC samples. This suggests that these genes may play a role in regulating HNSC on an immunological level. KEGG analysis results further support this hypothesis: TP53, PTEN, KRAS, and HRAS hub genes were enriched in the "Endometrial cancer, thyroid cancer, bladder cancer, and melanoma" etc., pathways. However, still there is a need to conduct more experiments for validating hub gene associations with immune infiltration in HNSC.

The expression of TP53, PTEN, KRAS, and HRAS hub genes in HNSC patients were simultaneously regulated by hsa-let-7a-5p miRNA, as identified by our study. Prior research reported dysregulation of hsa-let-7a-5p in various cancers such as breast cancer, bladder cancer, glioblastoma, and lung cancer hsa-let-7a-5p [67-69]. However, any tumor suppressor or tumor-causing role of hsa-let-7a-5p in HNSC has not yet bee reported. Therefore, exploration of the hsa-let-7a-5p oncogenic role in HNSC development with further biologic experiments will be highly valuable.

Conclusion

The current research disclosed a significant module and subsequently denoted crucial ferroptosis driver hub genes (TP53, PTEN, KRAS, and HRAS) as valuable diagnostic and pro gnostic biomarkers for HNSC patients. Bioinformatics, RNA-seq, and targeted bisulfite-seq based expression, methylation survival, and clinical variable analyses showed that TP53, PTEN, KRAS, and HRAS hub genes were significantly overexpressed and correlated to the poor survival of HNSC. Further investigation is necessary to fully elucidate the role of these hub genes in the development of HNSC.

Acknowledgements

The authors extend their appreciation to the Researchers Supporting Project number (RSPD2023R725) King Saud University, Riyadh, Saud Arabia.

Disclosure of conflict of interest

None.

Address correspondence to: Muhammad Jamil, PARC Arid Zone Research Centre, Dera Ismail Khan 29050, Pakistan. E-mail: jamilmatrah@gmail.com

References

[1] Bjordal K, Hammerlid E, Ahlner-Elmqvist M, de Graeff A, Boysen M, Evensen JF, Biorklund A, de Leeuw JR, Fayers PM, Jannert M, Westin T and Kaasa S. Quality of life in head and neck cancer patients: validation of the European Organization for Research and Treatment of Cancer Quality of Life Questionnaire-H&N35. Clin Oncol 1999; 17: 1008-1019.

[2] Singh M, Shah PP, Singh AP, Ruwali M, Mathur N, Pant MC and Parmar D. Association of genetic polymorphisms in glutathione S-transferases and susceptibility to head and neck cancer. Mutat Res 2008; 638: 184-194.

[3] Ma F, Laster K and Dong Z. The comparison of cancer gene mutation frequencies in Chinese and U.S. patient populations. Nat Commun 2022; 13: 5651.

[4] Papenberg BW, Allen JL, Markwell SM, Interval ET, Montague PA, Johnson CJ and Weed SA. Disparate survival of late-stage male oropharyngeal cancer in Appalachia. Sci Rep 2020; 10: 11612.

[5] Kubrak C, Olson K and Baracos VE. The head and neck symptom checklist©: an instrument to evaluate nutrition impact symptoms effect on energy intake and weight loss. Support Care Cancer 2013; 21: 3127-3136.

[6] Ma B, Meng F, Yan G, Yan H, Chai B and Song F. Diagnostic classification of cancers using extreme gradient boosting algorithm and multi-omics data. Comput Biol Med 2020; 121: 103761.

[7] Latunde-Dada GO. Ferroptosis: role of lipid peroxidation, iron and ferritinophagy. Biochim Biophys Acta Gen Subj 2017; 1861: 1893-1900.

[8] Su LJ, Zhang JH, Gomez H, Murugan R, Hong X, Xu D, Jiang F and Peng ZY. Reactive oxygen species-induced lipid peroxidation in apoptosis, autophagy, and ferroptosis. Oxid Med Cell Longev 2019; 2019: 5080843.

[9] Xu T, Ding W, Ji X, Ao X, Liu Y, Yu W and Wang J. Molecular mechanisms of ferroptosis and its role in cancer therapy. J Cell Mol Med 2019; 23: 4900-4912.

[10] Xu S, He Y, Lin L, Chen P, Chen M and Zhang S. The emerging role of ferroptosis in intestinal disease. Cell Death Dis 2021; 12: 289.

[11] Chen X, Comish PB, Tang D and Kang R. Characteristics and biomarkers of ferroptosis. Front Cell Dev Biol 2021; 9: 637162.

[12] Lin Y, Dong Y, Liu W, Fan X and Sun Y. Pan-cancer analyses confirmed the ferroptosis-related gene SLC7A11 as a prognostic biomarker for cancer. Int J Gen Med 2022; 15: 2501-2513.
[13] Lu R, Li Z and Yin S. Constructing a ferroptosis-related long non-coding RNA signature to predict the prognostic of head and neck squamous cell carcinoma patients by bioinformatic analysis. Biochem Genet 2022; 60: 1825-1844.
[14] Szklarczyk D, Gable AL, Nastou KC, Lyon D, Kirsch R, Pyysalo S, Doncheva NT, Legeay M, Fang T, Bork P, Jensen LJ and von Mering C. The STRING database in 2021: customizable protein-protein networks, and functional characterization of user-uploaded gene/measurement sets. Nucleic Acids Res 2021; 49: D605-D612.
[15] Shannon P, Markiel A, Ozier O, Baliga NS, Wang JT, Ramage D, Amin N, Schwikowski B and Ideker T. Cytoscape: a software environment for integrated models of biomolecular interaction networks. Genome Res 2003; 13: 2498-2504.
[16] Chin CH, Chen SH, Wu HH, Ho CW, Ko MT and Lin CY. cytoHubba: identifying hub objects and sub-networks from complex interactome. BMC Syst Biol 2014; 8 Suppl 4: S11.
[17] Chandrashekar DS, Bashel B, Balasubramanya SAH, Creighton CJ, Ponce-Rodriguez I, Chakravarthi BVSK and Varambally S. UALCAN: a portal for facilitating tumor subgroup gene expression and survival analyses. Neoplasia 2017; 19: 649-658.
[18] Tang Z, Li C, Kang B, Gao G, Li C and Zhang Z. GEPIA: a web server for cancer and normal gene expression profiling and interactive analyses. Nucleic Acids Res 2017; 45: W98-W102.
[19] Tang G, Cho M and Wang X. OncoDB: an interactive online database for analysis of gene expression and viral infection in cancer. Nucleic Acids Res 2022; 50: D1334-D1339.
[20] Park SJ, Yoon BH, Kim SK and Kim SY. GENT2: an updated gene expression database for normal and tumor tissues. BMC Med Genomics 2019; 12 Suppl 5: 101.
[21] Koch A, De Meyer T, Jeschke J and Van Criekinge W. MEXPRESS: visualizing expression, DNA methylation and clinical TCGA data. BMC Genomics 2015; 16: 636.
[22] Gao J, Aksoy BA, Dogrusoz U, Dresdner G, Gross B, Sumer SO, Sun Y, Jacobsen A, Sinha R, Larsson E, Cerami E, Sander C and Schultz N. Integrative analysis of complex cancer genomics and clinical profiles using the cBioPortal. Sci Signal 2013; 6: pl1.
[23] Thul PJ and Lindskog C. The human protein atlas: a spatial map of the human proteome. Protein Sci 2018; 27: 233-244.
[24] Xu Y, Wang X, Huang Y, Ye D and Chi P. A LASSO-based survival prediction model for patients with synchronous colorectal carcinomas based on SEER. Transl Cancer Res 2022; 11: 2795-2809.
[25] Li T, Fan J, Wang B, Traugh N, Chen Q, Liu JS, Li B and Liu XS. TIMER: a web server for comprehensive analysis of tumor-infiltrating immune cells. Cancer Res 2017; 77: e108-e110.
[26] Huang DP, Zeng YH, Yuan WQ, Huang XF, Chen SQ, Wang MY, Qiu YJ and Tong GD. Bioinformatics analyses of potential miRNA-mRNA regulatory axis in HBV-related hepatocellular carcinoma. Int J Med Sci 2021; 18: 335-346.
[27] Freshour SL, Kiwala S, Cotto KC, Coffman AC, McMichael JF, Song JJ, Griffith M, Griffith OL and Wagner AH. Integration of the drug-gene interaction database (DGIdb 4.0) with open crowdsource efforts. Nucleic Acids Res 2021; 49: D1144-D1151.
[28] Rio DC, Ares M Jr, Hannon GJ and Nilsen TW. Purification of RNA using TRIzol (TRI reagent). Cold Spring Harb Protoc 2010; 2010: pdb.prot5439.
[29] Livak KJ and Schmittgen TD. Analysis of relative gene expression data using real-time quantitative PCR and the 2(-Delta Delta C(T)) method. Methods 2001; 25: 402-408.
[30] Jafri HSMO, Mushtaq S and Baig S. Detection of Kras gene in colorectal cancer patients through liquid biopsy: a cost-effective method. J Coll Physicians Surg Pak 2021; 31: 1174-1178.
[31] Sadia H, Bhinder MA, Irshad A, Zahid B, Ahmed R, Ashiq S, Malik K, Riaz M, Nadeem T, Ashiq K and Akbar A. Determination of expression profile of p53 gene in different grades of breast cancer tissues by real time PCR. Afr Health Sci 2020; 20: 1273-1282.
[32] Ioffe YJ, Chiappinelli KB, Mutch DG, Zighelboim I and Goodfellow PJ. Phosphatase and tensin homolog (PTEN) pseudogene expression in endometrial cancer: a conserved regulatory mechanism important in tumorigenesis? Gynecol Oncol 2012; 124: 340-346.
[33] Tetsu O, Phuchareon J, Chou A, Cox DP, Eisele DW and Jordan RC. Mutations in the c-kit gene disrupt mitogen-activated protein kinase signaling during tumor development in adenoid cystic carcinoma of the salivary glands. Neoplasia 2010; 12: 708-717.
[34] Kim TK. T test as a parametric statistic. Korean J Anesthesiol 2015; 68: 540-546.
[35] Kim HY. Statistical notes for clinical researchers: chi-squared test and Fisher's exact test. Restor Dent Endod 2017; 42: 152-155.
[36] Schubert AD, Channah Broner E, Agrawal N, London N, Pearson A, Gupta A, Wali N, Seiwert TY, Wheelan S, Lingen M, Macleod K, Allen H,

Chatterjee A, Vassiliki S, Gaykalova D, Hoque MO, Sidransky D, Suresh K and Izumchenko E. Somatic mitochondrial mutation discovery using ultra-deep sequencing of the mitochondrial genome reveals spatial tumor heterogeneity in head and neck squamous cell carcinoma. Cancer Lett 2020; 471: 49-60.

[37] Chen J, Li X, Ge C, Min J and Wang F. The multifaceted role of ferroptosis in liver disease. Cell Death Differ 2022; 29: 467-480.

[38] Lu R, Li Z and Yin S. Constructing a ferroptosis-related long non-coding RNA signature to predict the prognostic of head and neck squamous cell carcinoma patients by bioinformatic analysis. Biochem Genet 2022; 60: 1825-1844.

[39] Soussi T. The p53 tumor suppressor gene: from molecular biology to clinical investigation. Ann N Y Acad Sci 2000; 910: 121-137; discussion 137-9.

[40] Khanna KK and Jackson SP. DNA double-strand breaks: signaling, repair and the cancer connection. Nat Genet 2001; 27: 247-254.

[41] Yu H, Guo P, Xie X, Wang Y and Chen G. Ferroptosis, a new form of cell death, and its relationships with tumourous diseases. J Cell Mol Med 2017; 21: 648-657.

[42] Dai C, Chen X, Li J, Comish P, Kang R and Tang D. Transcription factors in ferroptotic cell death. Cancer Gene Ther 2020; 27: 645-656.

[43] Chen GQ, Benthani FA, Wu J, Liang D, Bian ZX and Jiang X. Artemisinin compounds sensitize cancer cells to ferroptosis by regulating iron homeostasis. Cell Death Differ 2020; 27: 242-254.

[44] Birsen R, Larrue C, Decroocq J, Johnson N, Guiraud N, Gotanegre M, Cantero-Aguilar L, Grignano E, Huynh T, Fontenay M, Kosmider O, Mayeux P, Chapuis N, Sarry JE, Tamburini J and Bouscary D. APR-246 induces early cell death by ferroptosis in acute myeloid leukemia. Haematologica 2022; 107: 403-416.

[45] Li J, Cao F, Yin HL, Huang ZJ, Lin ZT, Mao N, Sun B and Wang G. Ferroptosis: past, present and future. Cell Death Dis 2020; 11: 88.

[46] Quan J, Bode AM and Luo X. ACSL family: the regulatory mechanisms and therapeutic implications in cancer. Eur J Pharmacol 2021; 909: 174397.

[47] Okahara F, Itoh K, Nakagawara A, Murakami M, Kanaho Y and Maehama T. Critical role of PICT-1, a tumor suppressor candidate, in phosphatidylinositol 3, 4, 5-trisphosphate signals and tumorigenic transformation. Mol Biol Cell 2006; 17: 4888-4895.

[48] Zhang L, Wang F, Li D, Yan Y and Wang H. Transferrin receptor-mediated reactive oxygen species promotes ferroptosis of KGN cells via regulating NADPH oxidase 1/PTEN induced kinase 1/acyl-CoA synthetase long chain family member 4 signaling. Bioengineered 2021; 12: 4983-4994.

[49] Tong X, Tang R, Xiao M, Xu J, Wang W, Zhang B, Liu J, Yu X and Shi S. Targeting cell death pathways for cancer therapy: recent developments in necroptosis, pyroptosis, ferroptosis, and cuproptosis research. J Hematol Oncol 2022; 15: 174.

[50] Tang D, Chen X, Kang R and Kroemer G. Ferroptosis: molecular mechanisms and health implications. Cell Res 2021; 31: 107-125.

[51] Zhao L, Zhou X, Xie F, Zhang L, Yan H, Huang J, Zhang C, Zhou F, Chen J and Zhang L. Ferroptosis in cancer and cancer immunotherapy. Cancer Commun (Lond) 2022; 42: 88-116.

[52] Tousignant KD, Rockstroh A, Poad BLJ, Talebi A, Young RSE, Taherian Fard A, Gupta R, Zang T, Wang C, Lehman ML, Swinnen JV, Blanksby SJ, Nelson CC and Sadowski MC. Therapy-induced lipid uptake and remodeling underpin ferroptosis hypersensitivity in prostate cancer. Cancer Metab 2020; 8: 11.

[53] Jančík S, Drábek J, Radzioch D and Hajdúch M. Clinical relevance of KRAS in human cancers. J Biomed Biotechnol 2010; 2010: 150960.

[54] Ye Z, Hu Q, Zhuo Q, Zhu Y, Fan G, Liu M, Sun Q, Zhang Z, Liu W, Xu W, Ji S, Yu X, Xu X and Qin Y. Abrogation of ARF6 promotes RSL3-induced ferroptosis and mitigates gemcitabine resistance in pancreatic cancer cells. Am J Cancer Res 2020; 10: 1182-1193.

[55] Koppula P, Zhuang L and Gan B. Cystine transporter SLC7A11/xCT in cancer: ferroptosis, nutrient dependency, and cancer therapy. Protein Cell 2021; 12: 599-620.

[56] Chen X, Kang R, Kroemer G and Tang D. Targeting ferroptosis in pancreatic cancer: a double-edged sword. Trends Cancer 2021; 7: 891-901.

[57] Xia X, Fan X, Zhao M and Zhu P. The relationship between ferroptosis and tumors: a novel landscape for therapeutic approach. Curr Gene Ther 2019; 19: 117-124.

[58] Mou Y, Wang J, Wu J, He D, Zhang C, Duan C and Li B. Ferroptosis, a new form of cell death: opportunities and challenges in cancer. J Hematol Oncol 2019; 12: 34.

[59] Kessler D, Gmachl M, Mantoulidis A, Martin LJ, Zoephel A, Mayer M, Gollner A, Covini D, Fischer S, Gerstberger T, Gmaschitz T, Goodwin C, Greb P, Häring D, Hela W, Hoffmann J, Karolyi-Oezguer J, Knesl P, Kornigg S, Koegl M, Kousek R, Lamarre L, Moser F, Munico-Martinez S, Peinsipp C, Phan J, Rinnenthal J, Sai J, Salamon C, Scherbantin Y, Schipany K, Schnitzer R, Schrenk A, Sharps B, Siszler G, Sun Q, Waterson A, Wolkerstorfer B, Zeeb M, Pearson M, Fesik SW and McConnell DB. Drugging an un-

druggable pocket on KRAS. Proc Natl Acad Sci U S A 2019; 116: 15823-15829.
[60] Yuan X, Larsson C and Xu D. Mechanisms underlying the activation of TERT transcription and telomerase activity in human cancer: old actors and new players. Oncogene 2019; 38: 6172-6183.
[61] Schott C, Graab U, Cuvelier N, Hahn H and Fulda S. Oncogenic RAS mutants confer resistance of RMS13 rhabdomyosarcoma cells to oxidative stress-induced ferroptotic cell death. Front Oncol 2015; 5: 131.
[62] Ju J, Song YN and Wang K. Mechanism of ferroptosis: a potential target for cardiovascular diseases treatment. Aging Dis 2021; 12: 261-276.
[63] Kinowaki Y, Taguchi T, Onishi I, Kirimura S, Kitagawa M and Yamamoto K. Overview of ferroptosis and synthetic lethality strategies. Int J Mol Sci 2021; 22: 9271.
[64] Imai H, Matsuoka M, Kumagai T, Sakamoto T and Koumura T. Lipid peroxidation-dependent cell death regulated by GPx4 and ferroptosis. Curr Top Microbiol Immunol 2017; 403: 143-170.
[65] Mantovani A, Allavena P, Sica A and Balkwill F. Cancer-related inflammation. Nature 2008; 454: 436-444.
[66] Hu X, Li YQ, Li QG, Ma YL, Peng JJ and Cai SJ. Osteoglycin-induced VEGF inhibition enhances T lymphocytes infiltrating in colorectal cancer. EBioMedicine 2018; 34: 35-45.
[67] Zhong G, Lou W, Yao M, Du C, Wei H and Fu P. Identification of novel mRNA-miRNA-lncRNA competing endogenous RNA network associated with prognosis of breast cancer. Epigenomics 2019; 11: 1501-1518.
[68] Pliakou E, Lampropoulou DI, Dovrolis N, Chrysikos D, Filippou D, Papadimitriou C, Vezakis A, Aravantinos G and Gazouli M. Circulating miRNA expression profiles and machine learning models in association with response to irinotecan-based treatment in metastatic colorectal cancer. Int J Mol Sci 2022; 24: 46.
[69] Simonian M, Sharifi M, Nedaeinia R, Mosallaie M, Khosravi S, Avan A, Ghayour-Mobarhan M, Bagheri H and Salehi R. Evaluation of miR-21 inhibition and its impact on cancer susceptibility candidate 2 long noncoding RNA in colorectal cancer cell line. Adv Biomed Res 2018; 7: 14.